As discussed in chapter 5, carbon spheres though appropriate for rolling action, have been sparsely studied. The main impediment in their frequent use is distortion in their shape under working conditions. Since metal nanoparticles have been invariably employed as friction and wear modifiers to the base oil, it appears fascinating to invigorate carbon spheres by nanoparticles. H. Song et al. have considered low shear strength and high ductility of environmentally benign silver nanoparticles to prepare the composite of silver nanoparticles with carbon spheres, Ag@C [H. Song et al. (2018)]. They have evaluated tribological properties of the composite using the ball on disk tribometer in water. Machines usually require oil-based lubricants instead of water. For having the applicability of the composite in oil-based lubricants, the Ag@C composite has been functionalized by an ionic liquid. In chapter 4, it has been described that ionic liquids possess distinctive properties such as non-volatility, innate polarity and high chemical and thermal stability. These are referred to as green solvents owing to negligible vapour pressure. Therefore, ionic liquids find pertinence in synthetic chemistry, specifically nanostructures. Enormous applications of ionic liquids have been realized in various fields, in general, catalysis [Migowski et al. (2007), Karakulina et al. (2016), Giacalone et al. (2016)] and lubrication, in particular. In the field of lubrication, these have been used as base lubricants [Jimenez et al. (2006), (2008), Saurin et al. (2016)]. Since ionic liquids are quite expensive, these are also recommended as additives to the lubricants [Zhang et al. (2012), Zhou et al. (2017), Zhou et al. (2009)].

The present chapter includes synthesis of carbon spheres and their composite by hydrothermal method and the assessment of their tribological activity on four-ball tester in polyethylene glycol (PEG-200). Functionalization of the composite, Ag@C

has been performed by the ionic liquid, 1-decyl 3-methyl imidazolium tetrafluoroborate (DMIMBF) to envision a categorical improvement in tribo-activity based on enhanced dispersibility in base oil PEG.

6.1. Materials & methods

6.1.1. Chemicals

Analytical Grade reagents glucose, ascorbic acid, silver nitrate and citric acid were used without further purification.

were used during present work.

6.1.2. Synthesis of Additives

6.1.2.1. Synthesis of carbon spheres and composite Ag@C

Carbon spheres were synthesized as described in chapter 5

For the synthesis of nanocomposite Ag@C, 10mL aqueous solution of silver nitrate ((0.1mole) was added to 25 mL aqueous solutions of each glucose (0.5 mole) and ascorbic acid (0.1 mole). The resulting solution was ultrasonicated for 30 min. The above solution was poured into a Teflon autoclave of 250 mL capacity. The temperature of the autoclave was kept at 180 ^{o}C for 12 h. When it comes down to room temperature, the reaction product was washed again and again with distilled water and finally with ethanol on a centrifuge machine. The product was ultrasonicated in absolute ethanol for 1h, and the solvent was evaporated till the dry composite Ag@C was obtained.

For the synthesis of nanocomposite Ag@C,

6.1.2.2. Synthesis of IL modified Ag@C

Ionic liquid (1-decyl 3-methyl imidazolium boron tetrafluoride) and Ag@C, both 0.5 gm each in 20mL DMF solvent, were ultrasonicated separately for 1h. The solutions were then mixed and stirred overnight at room temperature. After removing the solvent DMF by rota vapour, the remaining solid product was dried *in vacuo*.

6.1.3. Tests for triboactivity

The blends of additives with PEG were prepared in different concentrations 0.25, 0.5, 0.75 and 1 % (w/v) using a magnetic stirrer at 40-50 ^{o}C for 2h and then sonicated for 1h.

6.2. Results and Discussion

6.2.1. Structural and Morphological Characteristics of the Additives

The carbon spheres, Ag@C composite and IL modified Ag@C have been synthesized successfully by hydrothermal method. Their characterization has been accomplished by XRD, FE-SEM, TEM/HR-TEM, IR, Raman and XPS techniques. Thermal stability of the additives has been studied by thermogravimetric analysis.

The FE-SEM images of carbon spheres exhibit the size in the range of 2.5-2.1 µm. **Fig. 6.1a** and **6.1b** illustrate FE-SEM images of Ag@C and IL-Ag@C composites, respectively. **Fig. 6.1a** reveals that although carbon spheres are little agglomerated, the spherical silver nanoparticles are visibly embedded on their surface. The figures exhibit spherical nanoparticles of around 30-40 nm size adhered on the carbon spheres (1.2-1.6 µm). The size of carbon spheres has decreased from 2.5-2.1 µm to 1.2-1.6 µm in the Ag@C composite. According to **Fig. 6.1b**, the composite of nanoparticles

and carbon spheres are wrapped effectively by IL. For the clarity of morphology, the TEM images of the composite are also being provided in **Fig. 6.1 c** and **d**. The size of silver nanoparticle was found to be around 30-40 nm from TEM images also. The SAED pattern of the composite shows crystalline silver presented in the inset of **Fig 6.1 c**.

The elemental composition of the composites Ag@C and IL-Ag@C could be acquired from the EDX spectrum. The presence of the elements, boron, nitrogen, oxygen and fluorine along with silver and carbon together establish the formation of the proposed composite. Furthermore, the atomic weight % data shown in **Fig. 6.1e** accredits its synthesis.

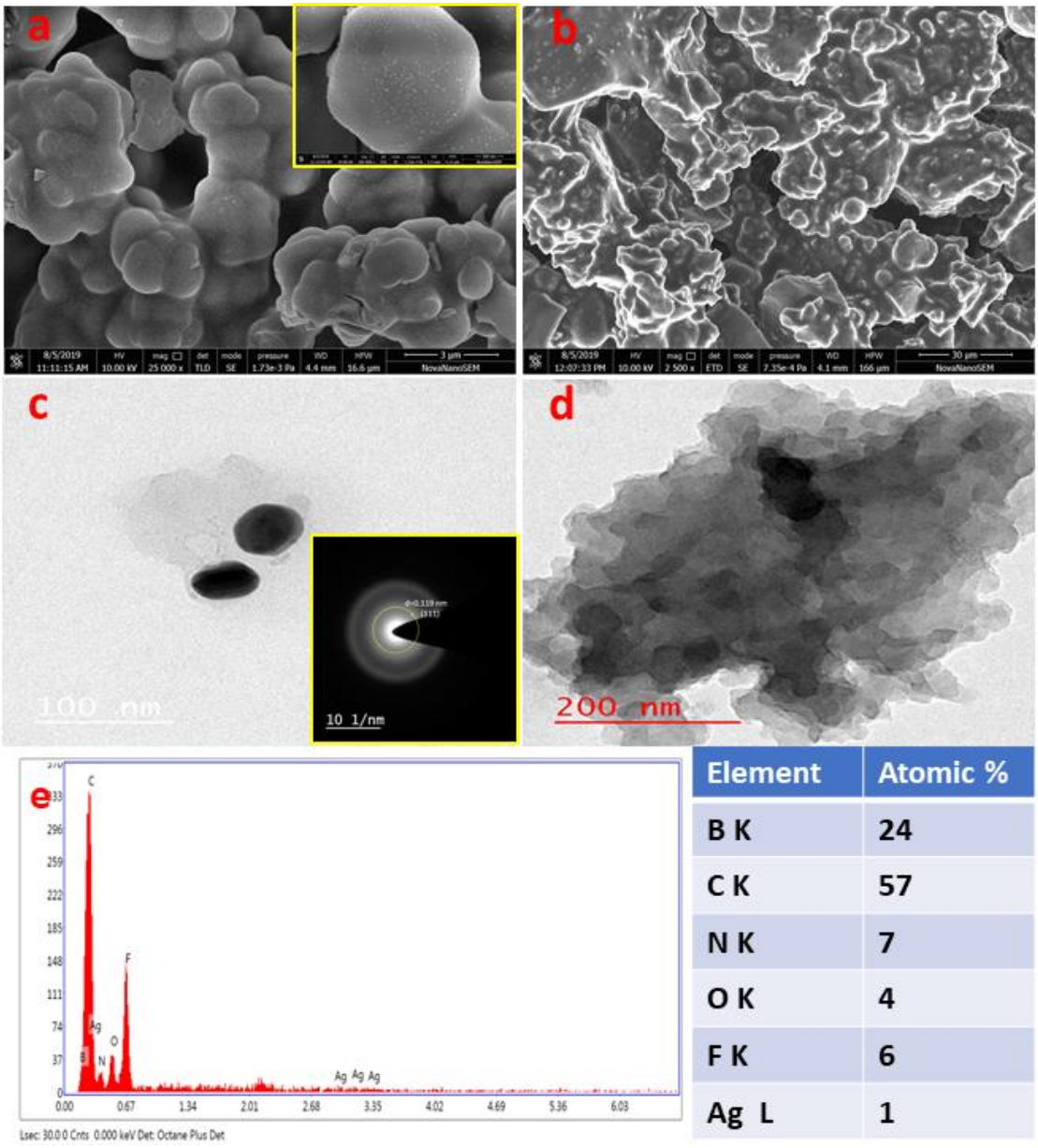

Element	Atomic %
B K	24
C K	57
N K	7
O K	4
F K	6
Ag L	1

Fig. 6.1. FE-SEM images of (a) Ag@C at resolution 3 µm, inset showing resolution 500 nm (b) IL-Ag@C, TEM images of (c) Ag@C, inset showing SAED pattern, (d) IL-Ag@C and (e) EDX spectra of IL-Ag@C

The crystal structure of carbon spheres, composite Ag@/C and IL modified Ag@C, was examined by X-ray diffraction (XRD) technique. The observed XRD patterns are presented in **Fig. 6.2**. The XRD pattern of carbon spheres exhibits one broad peak in the range of 10–35^{o} indicating amorphous carbon. The characteristic peaks of silver nanoparticles in the Ag@C composite display at 37.83, 43.93, 64.17 and 77.27^{o} following (111), (200), (220) and (311) planes respectively (JCPDS Card No. 87-0597) [Song et al. (2018)] and the broad peak in the range 10–35^{o} corresponds to amorphous carbon (JCPDS 75-2078). However, in IL modified Ag@C composite position of the peaks owing to silver nanoparticles and amorphous carbon remains almost unchanged, but their intensity is substantially reduced. The lowering of intensity signifies reduced crystallinity due to the presence of the ionic liquid.

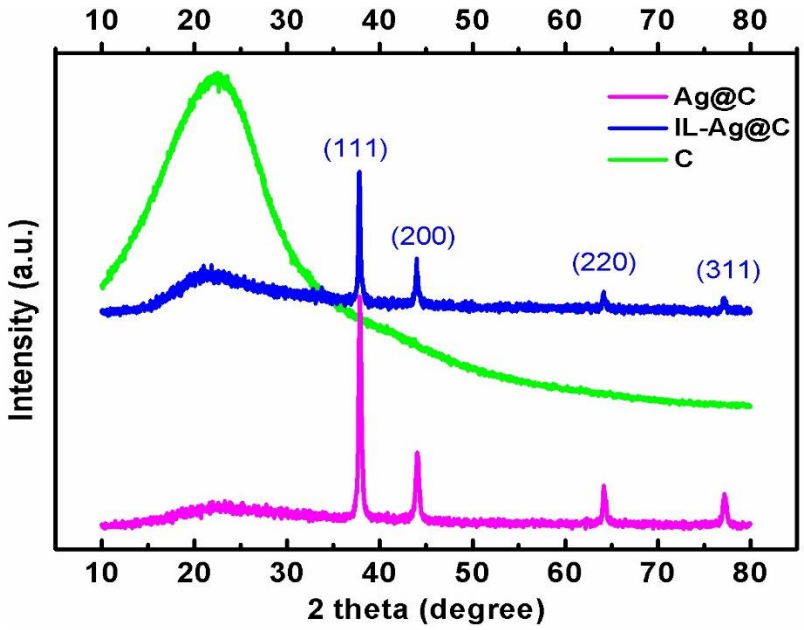

Fig. 6.2. XRD patterns of as-prepared Carbon spheres, Ag@C and IL-Ag@C composite

The FTIR spectra of carbon spheres, IL, Ag@C and IL-Ag@C, are given in **Fig. 6.3 a**. The figure shows a strong and broad absorption peak at 3435 cm^{-1} due to the stretching vibration of the OH group. The IR spectrum of IL (DMIM-BF_4) clearly shows two bands at 3089 and 3143 cm^{-1} assignable to the ring NC(H)NCH stretching and the ring HCCH symmetric stretching modes respectively. The symmetric ($\nu_s CH_2$) and asymmetric stretching vibrations ($\nu_{as} CH_2$) of the methylene groups were identified at 2865 and 2932 cm^{-1} indicating chain conformation. The bands appearing at 1710 cm^{-1} and 1620 cm^{-1} are characteristic peaks of C=O and C=C vibrations, respectively. Besides, the peaks in the region 1000 to 1400 cm^{-1} were attributed to C–OH stretching and OH bending vibrations of the residual hydroxyl groups on the surfaces of carbon spheres and Ag@C composite. Indeed, a strong peak at 1571 cm^{-1} is associated with the ring in plane symmetric, CH_3(N) and CH_2(N) stretching modes. Finally, ν B-F of tetrafluoroborate anion is observed at 1059 cm^{-1} [Hodyna et al. (2016)]

TGA analyses were conducted to study thermal stability and the weight changes corresponding to physical/chemical reactions occurring on increasing the temperature from 30 to 800^{o}C. **Fig. 6.3b** shows % weight loss against temperature for Ag@C and IL-Ag@C. For Ag@C weight loss below 300^{o}C was around 5% only, which may be due to desorption of the moisture and some less stable organic components containing oxygen. Beyond that, it decomposes up to 800^{o}C showing huge weight loss 62%, which may be due to loss of stable organic species. In case of the composite IL-Ag@C, the observed weight loss 4% up to 150^{o}C may be ascribed to desorption of moisture along with the removal of some volatile organic groups. After that, it

continuously decomposes up to 800°C with 44% weight loss associated with the expulsion of comparatively much stabler functional groups [Song et al. (2018)].

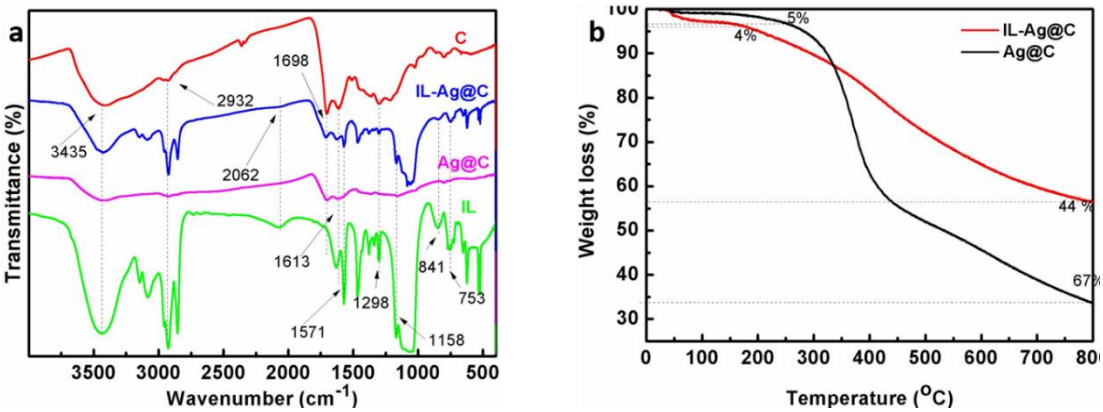

Fig. 6.3. (a) IR spectra of the synthesized additive C, IL, Ag@C and IL-Ag@C and (b) TGA analysis of the Ag@C and IL-Ag@C

Fig. 6.4 exhibits the Raman spectra of Ag@C and IL-Ag@C composite. The D and G bands are observed at 1354 and 1579 cm^{-1}respectively [Song et al. (2018), Wang et al. (2009)]. The ratio of intensities of D and G bands, I_D /I_G, is a measure of defects, sp^3 carbon atoms in a network of sp^2 graphitic carbon atoms. For Ag@C the ratio is 0.90, which increases to 0.93 in case of IL-Ag@C, the increased value of I_D /I_G approves the presence of a lesser graphitic character in IL-Ag@C.

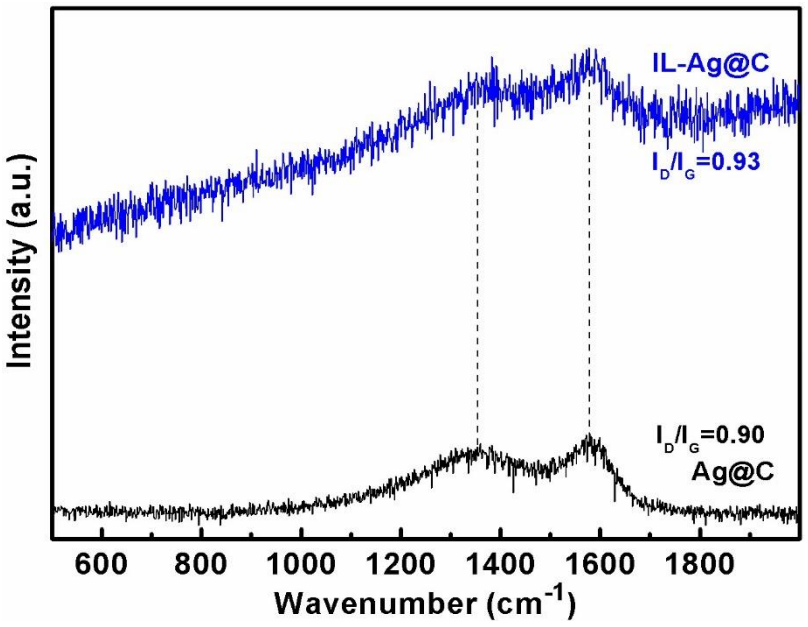

Fig. 6.4. Raman spectra of Ag@C and IL-Ag@C composite

X-ray photoelectron spectroscopy (XPS) was accomplished to confirm the chemical structure of the composite IL-Ag@C. **Figs. 6.5a-6.5e** show the best-fitted deconvoluted core level spectra with the help of peak fit software. The core-level spectrum of C 1s, presented in **Fig. 6.5a** produced three peaks at binding energies 284.8, 285.4 and 286.7 eV corresponding to C-C, C-N and C=O bonds respectively. **Fig. 6.5b** illustrates Ag 3d core level spectrum exhibiting two peaks at 368.8 and 372.15 eV binding energies attributable to Ag $3d_{3/2}$ and Ag $3d_{5/2}$ respectively. The core-level spectra of B 1s, **Fig. 6.5c** shows two peaks at binding energy 193.8 and 194.4 eV for B-O and B-F bonds respectively. The two peaks observed in N1s spectra, **Fig. 6.5d** at the binding energy 398.8 and 399.3 eV correspond to sp^2 and sp^3 C-N bonds respectively. The core-level spectra of F 1s, **Fig. 6.5e** shows a peak at 685 eV due to the B-F bond of the BF_4 anion of the ionic liquid DMIMBF. The survey

spectrum, **Fig. 6.5f** reveals peaks at 191.6, 283, 371.25, 398.4, 530.28 and 683 eV corresponding to the elements, B, C, Ag, N, O and F respectively. Presence of these elements authenticates the formation of the composite IL-Ag@C. Based on XPS data, it may be stated that ionic liquid is present along with Ag@C in the synthesized composite validating FE-SEM/TEM images which show ionic liquid wrapped around Ag@C.

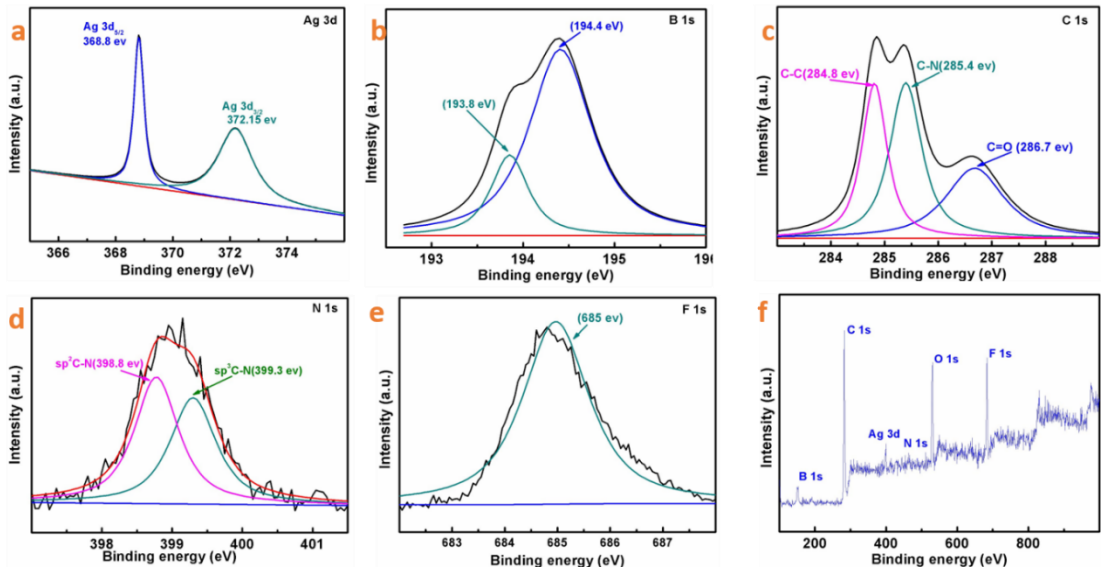

Fig. 6.5. Deconvoluted XPS images of IL-Ag@C composite: (a) C 1s, (b) Ag 3d, (c) B 1s, (d) N 1s (e) F 1s core-level spectra and (f) XPS survey spectra

6.2.2. Tribological Properties

6.2.2.1. Dispersion Stability of Nanofluids in a Base Oil

UV/visible spectroscopy was employed for determination of dispersion stability of the studied additives. The admixtures (0.5% w/v) were diluted ten times, and their absorbance values were recorded in the region 200-600 nm at six-hour intervals up to forty-eight hours. In the inset, the characteristics of absorbance values for dispersion

of IL-Ag@C at 218 nm from zero to 48 hours at six-hour intervals have been displayed. As expected, the absorbance drops with time within the tested period. **Fig. 6.6a** illustrates the relative absorbance of all the admixtures against settling time. The relative absorbance decreases almost continuously with time, usually for all additives. However, the decrease is a little gradual in case of IL-Ag@C after 24 h. It is apparent from Fig. 6a that the extent of decrease in relative absorbance declines from carbon spheres to IL-Ag@C through plain IL and Ag@C. All the additives have adequate stability as the relative absorbance decreases from 1.0 and reaches up to 0.35 in case of carbon spheres, 0.45 for plain ionic liquid, 0.48 for Ag@C finally 0.56 for IL-Ag@C. **Fig. 6.6b** presents direct photographs of base oil and its admixtures in the beginning and after 48 hours divulging their stability.

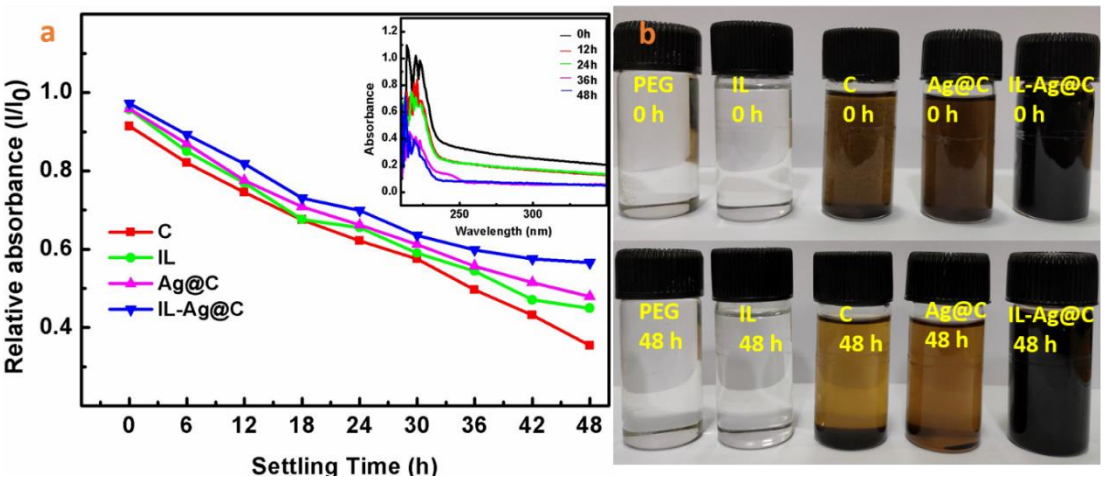

Fig. 6.6. (a) Dispersion stabilities of base oil containing carbon spheres, IL, Ag@C and IL-Ag@C composites studied by UV−vis spectrophotometry (b) Optical photographs of additives dispersed in base oil within 48 h

6.2.2.2. Additive optimization

The concentration of the additives was optimized by determining the size of wear scar diameter (MWD) in the presence of their concentrations, 0.00, 0.25, 0.5, 0.75 and 1% w/v in base lube according to ASTM D4172 test conditions. The variation of MWD with the concentration of the tested additives is shown in **Fig. 6.7**. It is evident from the figure that the additives are tribologically active at all the tested concentrations as there is a remarkable decrease in wear scar diameter from the base lube in every case. At 0.25%w/v concentration, there is a sharp decrease in MWD for all the additives. When concentration increases to 0.5 % w/v, the diminution in MWD is maximum for each of the additives. At the next concentration, 0.75% w/v, an increase in MWD is perceptible, which continues to be stable for the last concentration, 1%w/v. The optimized concentration for different additives stands as 0.5%w/v. It is noticeable from **Fig. 6.7** that in the concentration versus MWD plots, IL-Ag@C throughout shows the best lubricity performance among all the tested additives.

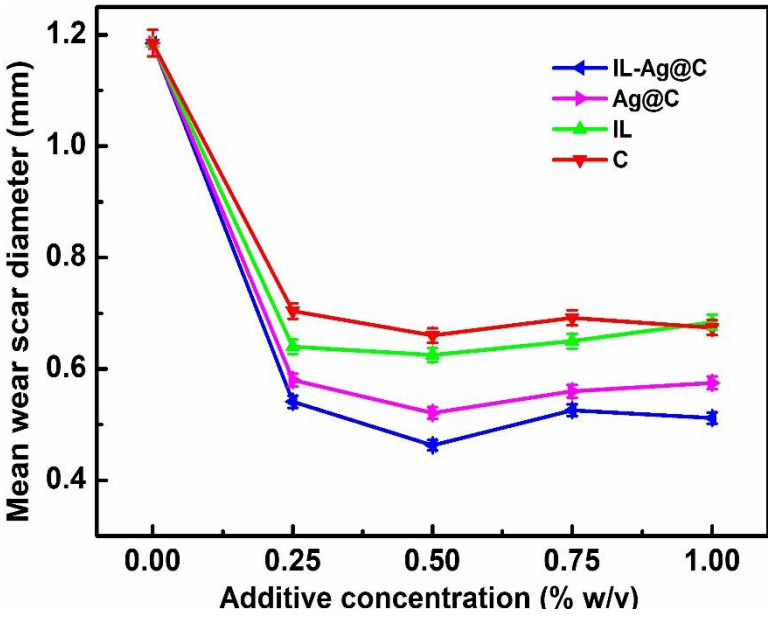

Fig. 6.7. Variation of mean wear scar diameter as a function of additive concentration (392 N, 60 min)

6.2.2.3. Antiwear and antifriction testing

Antiwear tests were conducted under ASTM D4172 test conditions. The test results, including MWD data and the average friction coefficient in PEG and its admixture with different additives, have been compiled in the form of a bar diagram, **Fig. 6.8 a**. The value of MWD in the presence of plain PEG is observed as 1.185. The effect of the decrease in size of carbon spheres in the composite is visible in MWD values and therefore in antiwear efficiency. There is an apparent boost in % reduction in MWD in the presence of carbon spheres (44), IL (47), Ag@/C (56) to IL-Ag@C (61). Thus, an enormous reduction in MWD values for the IL-modified Ag@C supports its tremendous tribological activity.

The average COF value for blank PEG, 0.12621 undergoes % reduction in a manner congruous to MWD for admixtures containing carbon spheres (28), IL (32), Ag@C (34) and IL-Ag@C (44). The reduction in the size of carbon spheres in the composite Ag@C has increased the antifriction efficiency. Wear and friction both are substantially diminished in the presence of the tested additives, especially IL-Ag@C. Thus, ionic liquid has played a significant role in improving the quality of *in situ* formed tribofilm.

The COF is directly related to the durability of machine parts; therefore, it is essential to see how it varies with time at a well-defined load. The variation of friction coefficient (COF) as a function of sliding time at 392 N load for blank polyethylene glycol (PEG) and its admixtures with the different additives are shown in **Fig 6.8 b**.

Initially, COF values are very high as there is no tribofilm on the surface. With the time the tribofilm is being formed; consequently, COF values are significantly reduced, attaining some stability. As per expectation, COF values are comparatively much higher for PEG base oil and arrive at the minimum value for its blend with IL-Ag@C. The low value of the friction coefficient is favourable for the persistence of machine components.

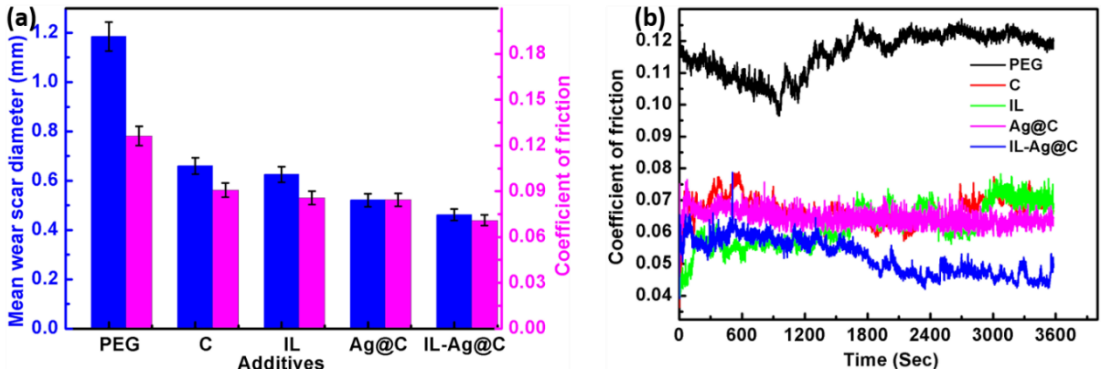

Fig. 6.8. (a) Comparative analysis of wear scar diameter and coefficient of friction (COF) of different additives at an optimum concentration of 0.5% (w/v) in PEG (392N, 60 min) (b) Variation of the coefficient of friction with time (392 N, 1200 rpm, 3600 sec) for the studied additives

6.2.2.4 Effect of load

Step loading test (ASTM D5183), for the running-in period, was performed at the outset under the conditions; optimum concentration of additives 392 N load, 600 rpm, 75^{o}C temperature, 60 min. Subsequently, the test was carried out for the steady-state by addition of 98 N load after every 10 min, and the frictional torque values were recorded until the seizure load is reached. The seizure of the tribo surfaces is the consequence of the failure of tribofilm to sustain the load. The obtained data are presented in **Fig. 6.9**. In the presence of base lube alone, the value of frictional torque

is considerably high, and seizure load is perceived at 1960N. At seizure load, tribofilm undergoes depletion affecting the steady-state and lubricant turns incompatible with carrying the load. The frictional torque values are comparatively better stabilized for different admixtures with stepwise addition of 98N load and passing the time. Seizure load is observed at 2646, 2744, 2842 and 3724 N in the presence of carbon spheres, IL, Ag@C and IL-Ag@C the respectively as additives. Thus, IL-Ag@C shows the best load-carrying capacity.

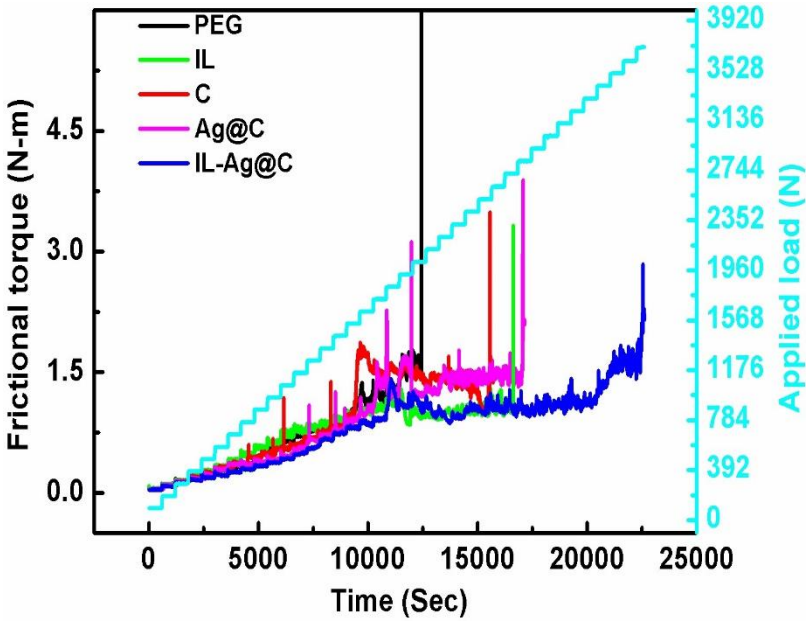

Fig. 6.9. Variation of frictional torque with time and step loading of 98 N after every 10 min of the test run for the optimized concentration of different additives

6.2.2.5. Frictional power loss

Frictional power loss was determined using data from antiwear tests in the following equation

$$P = \mu N.r.\ \pi dn/60 \qquad 6.1$$

Where, P is the frictional power loss ($N.m.s^{-1}$); N is contact load on three balls, and r is the frictional radius, d is frictional diameter and n= 1200 rpm. Substituting all values in Eq. [1], the frictional power loss

$$P = 3.6 \times 2.07 \times \mu\ (MJ) \qquad 6.2$$

Table 6.1: Loss of frictional power measured of different additives at an optimized concentration of 0.5 % (w/v) in PEG

S.N.	Additives	Power consumption (MJ)	Reduction in Power consumption	% Reduction in Power consumption
1.	PEG	0.941	----------	----------
2.	C	0.677	0.264	28.1
3.	IL	0.638	0.303	32
4.	Ag@C	0.628	0.313	33.3
5.	IL-Ag@C	0.529	0.414	43.8

The frictional losses are inherently associated with longevity of machine components. Concerted efforts are being made to minimize frictional losses somehow and thus enhance the working efficiency of machine components. The frictional power losses are shown in **Table 6.1** in the presence of an optimum concentration of the different additives. The frictional power loss value in the presence of plain PEG was observed as 0.94 MJ. Its blends with different additives cause a severe reduction in the frictional power loss. As apparent from the table, maximum reduction, 44% was

achieved for the additive IL-Ag@C. It shows that ionic liquid modified Ag@C composite acts as excellent energy saviour [Rawat et al. (2019)].

6.2.3. Morphological studies of the worn surface

Use has been made of the surface techniques, AFM and SEM for studying the morphology and surface properties of the wear scar of the base oil (PEG) and its blends with additives after ASTM D4172 test. In the presence of the blank base lube, the surface seems to be much deteriorated. The SEM micrographs in the presence of carbon nanospheres, ionic liquid, Ag@C and IL-Ag@C as additives to the base oil are shown respectively in **Figs. 6.10 (a-d)**. The order of smoothness of the surface exactly matches the values of MWD (shown in the inset) obtained from ASTM D4172 test. The finest surface was observed when IL-Ag@C was used as an additive.

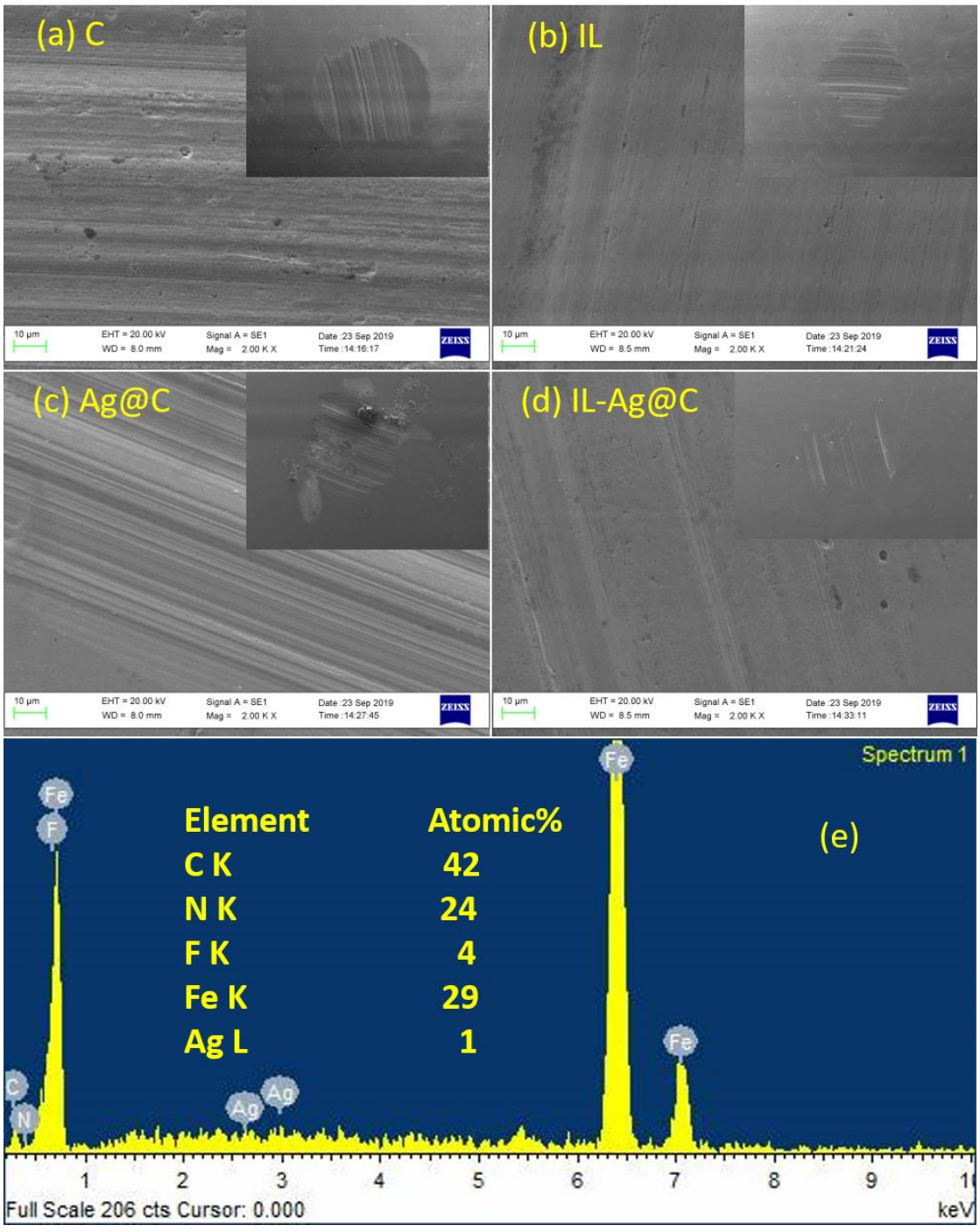

Fig. 6.10. SEM micrographs (Magnification 200X and 2.00kX) of the worn surface of a steel ball of the additives in PEG (a) C (b) IL (C) Ag@C and (d) IL-Ag@C at 392 N load 60 min test duration and (e) EDX results for the worn surface of tested specimen balls lubricated with IL-Ag@C

Besides silver, carbon and iron, the elements, nitrogen and fluorine are also detected in the EDX analysis of the worn surface in the presence of base oil with IL-Ag@C additive, **Fig. 6.10e**. Indeed, the source of nitrogen and fluorine is the ionic liquid. Boron of the ionic liquid could not be detected because of the minimal size. Thus, it may be convincingly argued that the adsorbed additive has been instrumental for enhancement in the triboactivity.

Contact mode AFM was used to reveal the roughness of the surface lubricated with carbon nanospheres, IL, Ag@C and IL-Ag@C as additives to base oil after ASTM D4172 test. The area and line roughness data (Sq and Rq) of the wear scar are laid out along with AFM images in **Fig. 6.11**. The observed roughness parameters for carbon spheres (Sq = 287 nm; Rq = 364 nm), IL (Sq = 211 nm; Rq = 126 nm) have undergone tremendous curtailment in case of the composites Ag@C (Sq = 141 nm; Rq = 122 nm) and IL-Ag@C (Sq =143 nm; Rq =42 nm) corroborating the other tribological data.

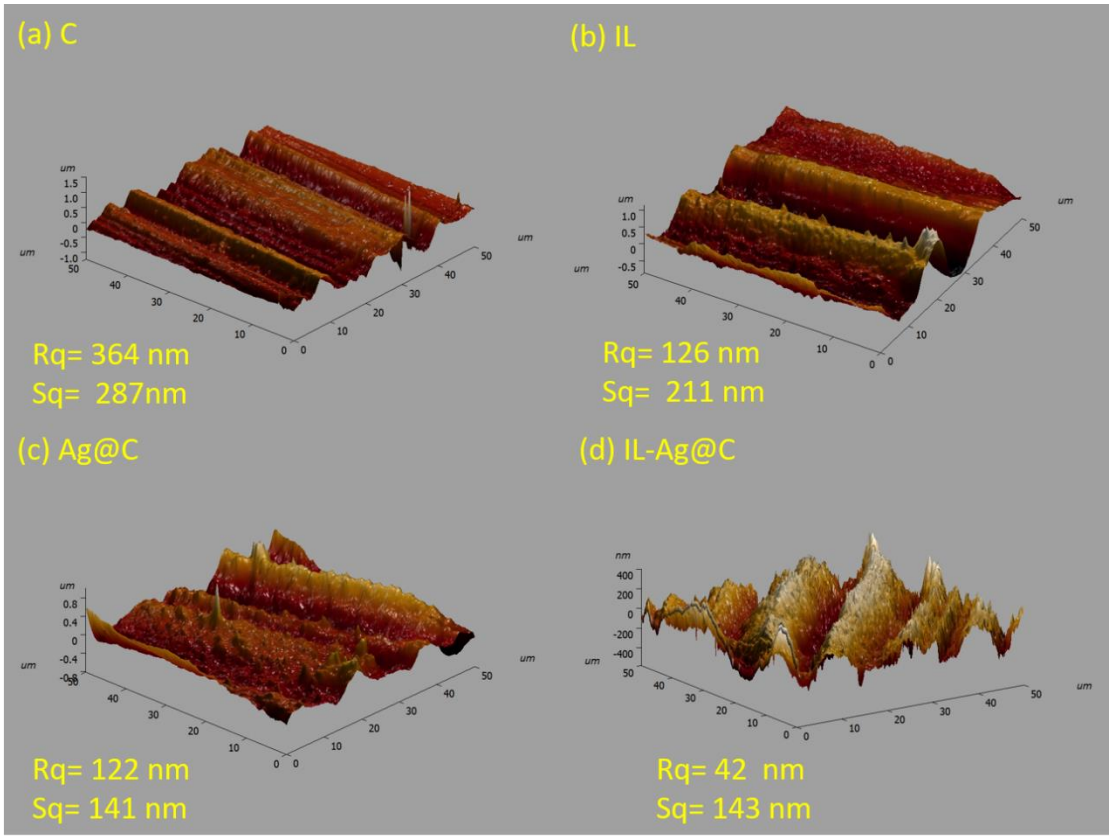

Fig. 6.11. *3D* AFM images of the worn steel surface lubricated with additives in PEG for 60 min test duration at a 392 N applied load (a) C, (b) IL, (c) Ag@C and (d) IL-Ag@C

6.2.4. Chemical composition of the tribofilm

The XPS spectra of the steel surface in the presence of IL-Ag@C was recorded after ASTM D4172 tribological test to identify the chemical composition of the tribofilm. The deconvoluted core- level XPS spectra with best-fitted curves (based on peak fit software) of C 1s, Ag 3d, B 1s, N 1s, F1s and Fe 2p of the worn surface are shown in **Fig. 6.12**. **Fig. 6.12a** shows the core-level spectrum of C 1s deconvoluted into four peaks. The first three peaks corresponding to C−C, N−C, C=O bonds are observed at binding energy 284.8, 285.4 and 286.7eV respectively. These peaks are almost at similar positions as observed for IL-Ag@C before the tribological test, **Fig. 6.5a**.

However, an additional peak is identified in **Fig. 6.12a** for C(O)O at the binding energy 288.8 eV. The XPS spectra of silver, **Fig. 6.12b** shows an almost negligible shift in the binding energies of Ag 3d5/2 and Ag 3d3/2 peaks as compared to **Fig. 6.5b**. The two peaks noted in the XPS spectra of boron at binding energy 189.2 and 191 eV are accorded with the B-N and B-C bonds respectively. The core-level spectra of N shows two peaks at the binding energy 399.5 and 400 eV due to the B-N and sp^3C-N bonds, respectively [Verma et al. (2019), Jaiswal et al. (2016)]. The core-level spectra of F shows a peak at 684.4 eV attributed to FeF_2 and another peak at 686 eV due to the B-F bond [Sanes et al. (2009)]. The iron of the steel surface may be oxidized to Fe_2O_3 under lubricating conditions. The observed peaks at 710.3 eV and 725 eV binding energy correspond to Fe^{2+}or Fe^{3+} oxides [Jaiswal et al. (2016), Ming et al. (2015)]. Thus, the XPS spectrum of the worn surface in the presence of IL-Ag@C indicates that the tribofilm is characterized by the presence of some *in situ* formed compounds like boron nitride, boron carbide along with iron II/ iron III oxides and fluorides. The best tribological activity of IL-Ag@C, therefore, can be mainly attributed to the formation of boron nitride and boron carbide in the tribofilm.

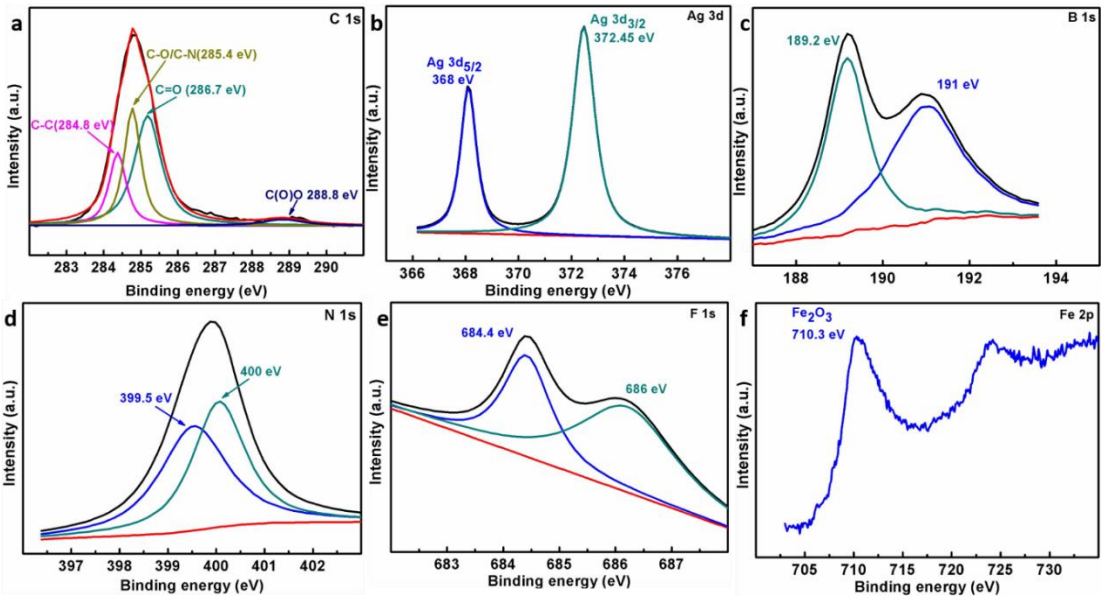

Fig. 6.12. Deconvoluted XPS images of the worn surface of IL-Ag@C composite: (a) C 1s, (b) Ag 3d, (c) B 1s, (d) N 1s, (e) F 1s and (f) Fe 2p core-level spectra

6.3. Conclusions

In summary, the Ag@C composite was synthesized successfully by hydrothermal method. It was further modified by ionic liquid to yield the composite IL-Ag@C. The standard techniques XRD, HR-TEM/TEM, FE-SEM, Raman and XPS, were employed to authenticate the formation of Ag@C and IL-Ag@C. The dispersion stability of blends of different additives C, IL, Ag@C and IL-Ag@C in PEG was determined from UV−visible spectra. It was found that the additives, in general, and IL-Ag@C, in particular, were sufficiently stable up to 48 h. The composite IL-Ag@C in PEG-200 has shown a marvellous reduction in wear and friction. The order of triboactivity of the additives in PEG is mentioned below:

$$\text{IL-Ag@C} > \text{Ag@C} > \text{IL} > \text{C} > \text{PEG}$$

The increase in triboactivity from carbon spheres to Ag@C could be ascribed to the reduction in their size in the composite. However, a further increase in triboactivity is

due to wrapping by the ionic liquid. The above order has been confirmed by surface morphology studies based on SEM and AFM. EDX analysis exhibits the presence of the elements N and F along with C and Ag on the sliding surface, indicating the role of ionic liquid in increasing the lubrication due to Ag@C. XPS studies revealed that the excellent triboactivity of IL-Ag@C might be accredited to boron nitride and boron carbide formed *in situ* during the evolution of tribofilm. Thus, the composite IL-Ag@C may be considered as an efficient wear and friction reliever under thin-film lubrication conditions.